Hogan Benjamin (Orcid ID: 0000-0002-0651-7065)

Pkd1 and *Wnt5a* genetically interact to control lymphatic vascular morphogenesis in mice

Tevin CY. Chau[1], Sungmin Baek[1], Baptiste Coxam[1], Renae Skoczylas[1], Maria Rondon-Galeano[1,2], Neil I. Bower[1], Elanor N. Wainwright[1], Steven A. Stacker[3,4,5], Helen M. Cooper[6], Peter A. Koopman[1], Anne K. Lagendijk[7], Natasha L. Harvey[8], Mathias François[1,9], Benjamin M. Hogan[1,2,6,10,*]

[1]Division of Genomics of Development and Disease, Institute for Molecular Bioscience, The University of Queensland, St Lucia, Queensland 4072, Australia.
[2] Organogenesis and Cancer Program, Peter MacCallum Cancer Centre, Melbourne, Victoria 3000, Australia.
[3] Tumour Angiogenesis and Microenvironment Program, Peter MacCallum Cancer Centre, 305 Grattan St, Melbourne, Victoria 3000, Australia.
[4] Department of Surgery, Royal Melbourne Hospital, The University of Melbourne, Parkville, Victoria3050, Australia.
[5] Sir Peter MacCallum Department of Oncology, University of Melbourne, Melbourne, Victoria 3010, Australia.
[6] The University of Queensland, Queensland Brain Institute, St Lucia, Queensland 4072, Australia.
[7]Division of Cell and Developmental Biology, Institute for Molecular Bioscience, The University of Queensland, St Lucia, Queensland 4072, Australia.
[8] Centre for Cancer Biology, University of South Australia and SA Pathology, Adelaide 5001, South Australia, Australia.
[9] David Richmond Laboratory for Cardiovascular Development; Gene Regulation and Editing Program, Centenary Institute, New South Wales 2050, Australia.
[10] Department of Anatomy and Physiology, University of Melbourne, Melbourne, Victoria 3000, Australia.

Author for correspondence:

Professor Ben Hogan
Organogenesis and Cancer Program,
Peter MacCallum Cancer Centre,
Melbourne, VIC 3000, Australia
E-mail: ben.hogan@petermac.org

Keywords: Polycystin 1, PC1; WNT5A; planar cell polarity; lymphangiogenesis, vascular, Polycystic kidney disease

Abstract

Background: Lymphatic vascular development is regulated by well-characterised signalling and transcriptional pathways. These pathways regulate lymphatic endothelial cell (LEC) migration, motility, polarity and morphogenesis. Canonical and non-canonical WNT signalling pathways are known to control LEC polarity and development of lymphatic vessels and valves. *PKD1*, encoding Polycystin-1, is the most commonly mutated gene in polycystic kidney disease but has also been shown to be essential in lymphatic vascular morphogenesis. The mechanism by which *Pkd1* acts during lymphangiogenesis remains unclear. Results: Here we find that loss of non-canonical WNT signalling components *Wnt5a* and *Ryk* phenocopy lymphatic defects seen in *Pkd1* knockout mice. To investigate genetic interaction, we generated *Pkd1*;*Wnt5a* double knockout mice. Loss of *Wnt5a* suppressed phenotypes seen in the lymphatic vasculature of *Pkd1*$^{-/-}$ mice and Pkd1 deletion suppressed phenotypes observed in *Wnt5a*$^{-/-}$ mice. Thus, we report mutually suppressive roles for *Pkd1* and *Wnt5a,* with developing lymphatic networks restored to a more wild type state in double mutant mice. This genetic interaction between *Pkd1* and the non-canonical WNT signalling pathway ultimately controls LEC polarity and the morphogenesis of developing vessel networks. Conclusion: Our work suggests that *Pkd1* acts at least in part by regulating non-canonical WNT signalling during the formation of lymphatic vascular networks.

Introduction

The lymphatic vasculature develops progressively in a process that involves cell specification, cell migration, cell proliferation and morphogenesis reviewed in [1]. In mice, precursor cells along the embryonic veins acquire lymphatic endothelial cell (LEC) fate via the activity of key transcription factors [2-4]. The specified LECs sprout out of the veins from approximately 10 days post coitum (dpc) and migrate throughout the embryo to form the lymphatic network [5,6]. Early lymphatic sprouting is known to be induced by vascular endothelial growth factor C (VEGFC), signalling through its receptor VEGFR3 [7]. Subsequent to sprouting, LECs organise, polarise and undergo coordinated cellular and tissue morphogenesis events before forming mature lymphatic vessel networks. These later cellular events controlling vessel morphogenesis and maturation remain to be fully understood.

A growing body of evidence has demonstrated that LEC polarisation and lymphatic vascular morphogenesis can be regulated by WNT signalling components and pathways in mice [8-12]. The non-canonical WNT/planar cell polarity (PCP) pathway is a highly conserved pathway that coordinates cell and organelle orientation, coordinated cell movements and tissue polarity during development. The PCP pathway is activated by the binding of several WNT ligands (including WNT4, WNT5A, WNT5B, WNT11 and WNT11B), to Frizzled (FZD) receptors and co-receptors; Receptor tyrosine kinase (RYK) and Rar-related orphan receptor (ROR) [13,14,]reviewed in [15]. Upon activation, various PCP core components, such as Van gogh-like (VANGL) and Cadherin EGF seven-pass G-type receptor (CELSR), are recruited to the activated receptors. These proteins in turn recruit downstream effectors, such as Dishevelled (DVL), Diversin (ANKRD6), and Prickle (PK), and generate asymmetry to establish cell polarity. Downstream, activation of factors such as RHO kinase or RAC1 influences cell migration and cell motility to co-ordinate tissue morphogenesis reviewed in [16]. Canonical WNT signalling occurs when WNT ligands bind to their cognate receptors, initiating the downstream interactions that lead to translocation of ß-catenin to the nucleus. This leads to downstream transcription driven by T-cell factor dependent transcription factors (TCFs) reviewed in [17].

The autosomal dominant polycystic kidney disease (ADPKD) gene *Polycystic kidney disease* (*Pkd1*), encodes the protein Polycystin-1 (PC1), that is mutated in as many as 85% of patients with polycystic kidney disease [18]. PC1 is a large 11 transmembrane protein with a long N-terminal extracellular region made up of multiple sub-domains and shown to play a role in mechanosensation [19-21]. PC1 localises to the primary cilium, apical membranes and the desmosomes in various cell types and its C-terminal tail binds to Polycystin-2 (PC2 encoded by Pkd2) [21,22]. PC2 is a calcium channel that is activated via PC1 function and influences downstream intracellular signalling events [21,23,24]. PC1 has been reported to

bind directly to core components of the non-canonical WNT/PCP pathway, PAR3 and aPKC, and to regulate cell polarity in kidney epithelia. This role in kidney tubules, regulates the normal intercalation of epithelial cells, tubular extension and morphogenesis [25]. PC1 can also influence Ca^{2+} dependent canonical WNT signalling and in *Xenopus* embryos *Pkd1* genetically interacts with *Wnt9a* and *Dishevelled* 2 [26].

We and others have found that mice mutant for *Pkd1*$^{-/-}$ display defects in lymphatic vascular morphogenesis [27,28]. *Pkd1*$^{-/-}$ mice display prominent oedema at 14.5 dpc that is typical in animals with lymphatic vascular defects. In the developing dermal lymphatic network, *Pkd1*$^{-/-}$ mice exhibit reduced lymphatic vessel branching and dilated/distended lymphatics as a result of the failure of endothelial cells within these vessels to polarise correctly in the direction of vessel sprouting [27,28]. Knockdown of *Pkd1* in cultured lymphatic endothelial cells also results in a loss of polarity during cell migration [28]. These earlier studies clearly demonstrated an unexpected role for the polycystic kidney disease gene *Pkd1* in lymphangiogenesis and identified it as a potential lymphatic disease gene. However, the precise pathway that *Pkd1* interacts with to control lymphatic vessel development has remained unexplored.

Here, we aimed to better understand the mechanism by which *Pkd1* regulates LEC polarity and lymphatic vascular morphogenesis. We first investigated the endothelial cell-autonomous role of *Pkd1* in valve development, which is known to be controlled by components of the canonical and non-canonical WNT/PCP pathways. We uncovered a requirement for *Pkd1* for normal lymphatic valve development. We then explored the roles of the non-canonical WNT/PCP components *Wnt5a* and *Ryk* in lymphatic development and uncovered phenotypes in knockout mice that were strikingly similar to *Pkd1* mutant phenotypes. Finally, we generated *Pkd1/Wnt5a* double knockout mice and found that these factors genetically interact during the regulation of LEC polarity, organisation of endothelial cells within developing vessels and in lymphatic vascular morphogenesis, being genetic suppressors of each other (a mutually suppressive relationship). Overall, these genetic studies suggest a role for *Pkd1* in the modulation of non-canonical WNT/PCP pathway signalling in lymphatic vascular development, likely similar to the developmental role of Pkd1 in the morphogenesis of kidney tubules during development.

Results

Pkd1 cell-autonomously regulates lymphangiogenesis and lymphatic valve development

We have previously reported a cell-autonomous role for *Pkd1* in lymphangiogenesis using *Sox18:GFP-Cre-ErT2(GCE)* to generate conditional *Pkd1* knockout mice [27]. In the previous study, *Sox18:GFP-Cre-*

ErT2(GCE);B6.129S4-Pkd1^{tm2Ggg}/J (*Pkd1$^{f/f}$)* mice showed subcutaneous lymphatic network defects but *Tie2:Cre;Pkd1$^{f/f}$* mice did not. To further validate previous findings, we here used *Cdh5:Cre-ErT2,* (which shows activity from 7.5dpc to adult vasculature [29,30]) and generated *Cdh5:CreERT2;Pkd1$^{f/f}$* mice (hereafter referred to as *Pkd1^{iECKO}*). During development, Cre activity was induced with serial tamoxifen injections at 9.5dpc, 10.5dpc and 11.5dpc. At 14.5dpc, we examined subcutaneous lymphatics for Prospero homeobox 1 (PROX1), Neuropilin 2 (NRP2) and Endomucin (EMCN) expression. *Pkd1^{iECKO}* embryos showed no marked subcutaneous oedema or morphological changes compared with their wild type siblings (**Figure 1A-B**). The subcutaneous blood vessel network was unaffected (**Figure 1C'-D', J-K**). However, the lymphatic network of *Pkd1^{iECKO}* embryos showed reduced complexity with fewer branch points and loops (**Figure 1C-D, G-H**). In the developing dermis, where lymphatics migrate from lateral locations towards the embryonic midline [31], the lymphatic sprouts of the *Pkd1^{iECKO}* embryos showed reduced medial migration and the lymphatic vascular front displayed a greater distance to the midline (**Figure 1I**). Furthermore, the dermal lymphatic sprouts were broader and showed a blunt-tipped morphology (**Figure 1E and F, L-M**). Combined with our previous work [27], this confirmed that PC1 functions in an endothelial cell-autonomous manner to regulate lymphatic vascular morphogenesis in the developing dermis.

To further study the role of PC1 in LEC polarity, we examined the formation of valves in the dermal lymphatic vasculature. The formation of dermal lymphatic valves requires the local up-regulation of Prox1 in valve-forming territories, typically at vessel branch points, this is followed by the polarisation and the reorientation of developing LECs. In 16.5dpc dermal lymphatics, we observed a marked reduction in valve forming territories in *Pkd1^{iECKO}* embryos, as determined by scoring regions of high Prox1 expression in the dermal network relative to the number of network branch points (**Figure 1L-N**). Reduced nuclear ellipticity is an indication of cells with reduced motility and a failure to polarise [5], suggesting a reduction in polarity or motility in *Pkd1^{iECKO}* LECs. We observed that the nuclei of the few lymphatic valves that did form in *Pkd1^{iECKO}* dermal lymphatics had reduced ellipticity compared with control embryos and LEC nuclei failed to reorient perpendicular to the vessel walls, indicative of reduced cell polarity in valve forming territories (**Figure 1L', M'**). Quantitatively, there were fewer polarised valves in 16.5dpc *Pkd1^{iECKO}* dermal lymphatics than in control embryos (**Figure 1O**).

To examine how PC1 regulates lymphatic valve formation in the mesentery, where valve formation has been better characterised reviewed in [1,32,]and [33], we injected tamoxifen at 15.5dpc, 16.5dpc, and 17.5dpc and examined mesenteric lymphatics in 18.5dpc embryos. In wild type siblings, valve LEC nuclei were polarised perpendicular to the lymphatic vessel walls with actin stress fibres aligned at the lymphatic valves in a stereotypical pattern (**Figure 1P and P"**). The *Pkd1^{iECKO}* valve LEC nuclei were

identifiable based on high levels of Prox1 expression and formed an initial ring, however the cells within these valve territories failed to orient perpendicular to the lymphatic vessel (**Figure 1Q-Q'**), and had less elongated nuclei (**Figure 1R**). Actin recruitment or organisation at the lymphatic valves was also reduced in *Pkd1*^{iECKO} embryos, as shown by a reduced ratio of valve-to-vessel actin fluorescent intensity (**Figure 1Q" and S**). Thus, *Pkd1/*PC1 endothelial cell-autonomously regulates the formation of lymphatic valves in the mesentery. The lymphatic valve phenotypes that we observed here and the randomised Golgi orientation in the dermal lymphatic sprouts previously reported [27] strongly suggested a loss of cell polarity in *Pkd1* mutants. The lymphatic valve phenotypes were also similar to valve phenotypes seen in published mouse models such as the *Fat4* conditional knockout mouse or the *Celsr1* mutant mouse, both impacting non-canonical WNT/PCP signalling mesenteric lymphatic valves [12,34]. Similarly, Prickle1, another PCP component, expresses at the lymphatic valve buttress, and *FOXC1/2* deletion leads to the mislocalisation of Prickle1 and lymphatic valve malformation [35].

The planar cell polarity pathway ligand WNT5A regulates lymphatic endothelial cell polarity during development

The LEC polarity phenotypes observed in *Pkd1*^{iECKO} and the previously described interaction between PC1 and PCP components in epithelial cells led us to further investigate the relationship between PC1 and the non-canonical WNT/PCP pathway using genetics. Previous studies have shown that a PCP ligand, WNT5A, is required for dermal lymphatic development [8,10]. These studies described lymphatic sprout morphology and structure in *Wnt5a*$^{-/-}$ embryos but polarity phenotypes in lymphatic network morphogenesis were not fully described.

We analysed the dermal lymphatics of *Wnt5a*$^{-/-}$ embryos at 13.5dpc and observed reduced network formation in the *Wnt5a*$^{-/-}$ dermal lymphatics (**Figure 2A-B**). *Wnt5a*$^{-/-}$ dermal lymphatics were dilated and the lymphatic sprouts failed to migrate towards the midline of the embryo (**Figure 2C-D**). In *Wnt5a*$^{-/-}$ mice, there was an increased number of cells in lymphatic vessels (measured along 150µm of the vessel starting at the leading vessel tips of lymphatic sprouts) and the LEC nuclei displayed reduced ellipticity compared with controls (**Figure 2E-F**). This suggested reduced cell polarity and a lack of LEC migration. To assess whether this phenocopies the *Pkd1*-knockout mice, we investigated LEC polarity more directly. In polarised endothelial cells, the Golgi aligns in the direction of migration, positioning between the nucleus and the direction of migration (**Figure 2I**). Lymphatic vascular mutants with disrupted polarity show a loss of this nuclear-Golgi polarisation in the direction of the embryonic midline [27,34]. We examined the polarity of LECs in *Wnt5a*$^{-/-}$ embryos by examining Golgi

(GOLPH4) localisation relative to the LEC nuclei (PROX1) and the midline (**Figure 2G-H'**). The Golgi body consistently aligned in the direction of migration in wild type sprouts, but alignment was more randomised and less directional in *Wnt5a*$^{-/-}$ mice (**Figure 2J-K**), indicating a loss of cell polarity in *Wnt5a*$^{-/-}$ LECs. These phenotypes further suggest that a loss of PCP signalling, polarity and convergence extension leads to abnormal lymphatic vessels in *Wnt5a*$^{-/-}$ mice. The blood vessel network displayed striking, abnormal endothelial cell clusters along the midline in *Wnt5a*$^{-/-}$ mice (**Figure 2A'-B'**) but there were no measurable differences in the number of branch points and loops in blood vessel networks at 13.5dpc (**Figure 2L-M**), a stage when wild type embryos were yet to form a dense blood vessel network spanning the embryonic midline. Overall, these phenotypes suggested that WNT5A, a PCP pathway ligand, regulates lymphangiogenesis by controlling cell polarity, displaying a similar but more severe phenotype than *Pkd1*^{iECKO} mice.

The planar cell polarity co-receptor Ryk regulates lymphangiogenesis during development

During PCP signalling, WNT5A binds to receptors, including FZD, ROR and RYK, to initiate downstream cellular processes reviewed in [16]. WNT5A enhances RYK and VANGL2 binding to establish cell polarity [36]. RYK and VANGL2 regulate PCP during mouse cochlea and neural tube development [37]. To further understand the role of PCP pathway components in lymphatic development, we assessed the role of the co-receptor RYK in lymphangiogenesis. *Ryk* knockout mice display classical PCP pathway phenotypes that include craniofacial and neural tube defects, and misoriented stereociliary bundles of sensory hair cells in the cochlea [37,38]. Upon examination of the dermal lymphatics, *Ryk*$^{-/-}$ embryos showed similar but milder lymphatic defects compared with *Wnt5a*$^{-/-}$ mice. The *Ryk*$^{-/-}$ mutant dermal lymphatic network had a marked reduction in branching (**Figure 3A-B**), increased vessel width (**Figure 3E**) and increased numbers of cells per vessel (scored as cell number per 100µm of vessel from the tips of lymphatic sprouts) (**Figure 3F**). The lymphatic sprouts displayed a stereotypical blunt-tipped and widened morphology (**Figure 3C-D**) and the nuclei at these lymphatic sprout tips were less elliptical in the *Ryk*$^{-/-}$ mutant (**Figure 3G**). Overall, this phenotype was consistent with a mild loss of polarity during lymphatic network morphogenesis. Interestingly, the blood vessel network was not affected in these mutants (**Figure 3A'-B', H-I**). Overall, this indicates that RYK, a WNT5A co-receptor, is also a regulator of lymphatic vascular morphogenesis during development.

***Pkd1* and *Wnt5a* genetically interact to control lymphatic endothelial cell polarity and lymphatic vessel morphogenesis of the dermal vasculature**

Given similar phenotypes in the absence of *Pkd1*, *Wnt5a* and *Ryk*, we hypothesised that *Pkd1* may modulate lymphatic vascular morphogenesis by interacting with the non-canonical WNT/PCP

signalling pathway. We used genetics to probe for an interaction at the level of vessel phenotype. We generated *Pkd1*$^{+/-}$*; Wnt5a*$^{+/-}$ double heterozygous mice (using a ubiquitous Pkd1-knockout model, not the iECKO model) and in-crossed the double carriers to examine the lymphatic networks for the various genotypes generated. We used a number of quantitative phenotypic measurements to analyse the dermal lymphatics of the 14.5dpc embryos.

As reported previously, both *Pkd1*$^{-/-}$ and *Wnt5a*$^{-/-}$ lymphatic networks had significantly wider lymphatic vessels (**Figure 4B-F',** quantification in **Figure 5A**). Strikingly, the loss of a single copy of *Wnt5a* modified the homozygous *Pkd1* mutant phenotype at the level of vessel width, suppressing the widened vessel phenotype and restoring a more wild type morphology to the network overall (**Figure 4I and J, Figure 5A**). Loss of a single copy of *Pkd1* did not modify the width of vessels in *Wnt5a* homozygous mutants (**Figure 4K-L, Figure 5A**). The developing dermal lymphatics of *Pkd1*$^{-/-}$*; Wnt5a*$^{-/-}$ double mutants were also significantly thinner than in *Pkd1*$^{-/-}$ or *Wnt5a*$^{-/-}$ mutant mice (**Figure 4G-H**), further revealing an unexpected partial phenotypic rescue. At the level of LECs per vessel (within 100µm from the tips of lymphatic sprouts), *Pkd1*$^{-/-}$*;Wnt5a*$^{-/-}$ embryos displayed fewer cells per vessel than in *Pkd1*$^{-/-}$ embryos and were therefore closer to a wild type control vessel (**Figure 4G-H, Figure 5B**). As these data may suggest a genetic interaction at the level of cell polarity and migration, we further quantified nuclear ellipticity in these vessels as a proxy for polarity and motility. *Pkd1*$^{-/-}$*;Wnt5a*$^{+/-}$ and *Pkd1*$^{-/-}$*;Wnt5a*$^{-/-}$ LEC nuclei were more elliptical than those quantified in the *Pkd1*$^{-/-}$ LEC nuclei (**Figure 4 B', D', F', H', J', L'** and **Figure 5C**). Finally, we assessed the number of LECs at the tips of leading vessels, as a measure of the blunt tip phenotype. Here we saw not just that loss of alleles of *Wnt5a* suppressed (or partially rescued) the *Pkd1* phenotype, but that loss of a single copy of *Pkd1* dominantly suppressed the *Wnt5a* phenotype as well (**Figure 4 B', D', F', H', J', L'** and **Figure 5D**).

We also examined the blood vessel network for genetic interaction. The blood vessel network had a reduced number of branch points in all mutant genotypes when compared with wild type embryos in medial and flank regions, likely due to subcutaneous oedema in these mutant embryos. However, there was no change or rescue of this phenotype in the double mutants (**Figure 4A', C', E', G', I', K'** and **Figure 5E**). This suggests that the genetic interaction described above is lymphatic restricted and blood vessel phenotypes are likely to be influenced by the sub cutaneous oedema that has been previously reported. We also examined the blood vessel networks between the various genotypes for numbers of loops but found no significant changes compared with wild type (**Figure 4A', C', E', G', I', K'** and **Figure 5F**).

Overall, this genetic interaction in lymphatic network morphogenesis between *Pkd1* and *Wnt5a* led to partial phenotypic rescue in the genotype combinations indicated above and provides genetic

evidence that *Pkd1* and *Wnt5a* regulate cell polarisation and vessel morphogenesis during lymphangiogenesis, likely by acting in the same genetic pathway.

Discussion

In this study, we show that *Pkd1*, *Wnt5a* and *Ryk* are important for lymphangiogenesis and LEC polarity. *Pkd1* regulates subcutaneous lymphatic network and valve formation endothelial cell-autonomously. The cell migration, elongation and orientation defects reported here and in earlier studies [27,28] suggest that *Pkd1* regulates lymphangiogenesis through controlling LEC polarity. WNT5A and RYK also regulate lymphangiogenesis, with reduced lymphatic network complexity in *Ryk* and *Wnt5a* mutants and loss of polarised Golgi body alignment and reduced nuclei elongation in *Wnt5a* mutants. To further probe the relationship between *Pkd1* and the non-canonical WNT/PCP ligand WNT5A, we generated double mutants and revealed a clear genetic interaction between *Pkd1* and *Wnt5a.* The loss of *Wnt5a* partially rescued (suppressed) the dermal lymphatic phenotypes caused by the loss of *Pkd1*, and in the case of the morphogenesis of vessel tips, vice versa. Overall, these findings report new phenotypes in *Pkd1*, *Wnt5a* and *Ryk* knockout mice and suggest that PC1 acts in the PCP pathway during lymphatic development.

Several studies have suggested the importance of the PCP pathway in lymphangiogenesis. FAT4, a component of the global PCP modules, is required for LEC polarisation and lymphatic development in mice and mutated in the inherited lymphoedema syndrome, Hennekam syndrome [34,39]. Lymphatic specific deletion of *Fat4* in mice results in lymphatic vessel networks with reduced branch points and increased vessel width. It also leads to reduced mesenteric lymphatic valve formation as does the loss of its ligand Dachsous1 [34,40]. LECs in lymphatic specific *Fat4* deletion mice are more rounded, and their Golgi bodies less aligned in the direction of migration and the nuclei [34]. Overall, these phenotypes are strikingly similar to those observed in *Pkd1* knockout mice. WNT5A, a ligand of the PCP pathway, is also required for dermal lymphatic morphogenesis [8,10]. *Wnt5a*-null mice have reduced numbers of dermal lymphatic capillaries but no difference in LEC proliferation [8]. Lymphatic vessels in *Wnt5a*-null mice are cyst-like, non-functional and blood-filled [10]. We examined these vessels at 13.5 dpc rather than 14.5 dpc in single mutant animals because of severe morphological defects in these mutants at later stages. These lymphatic vessels show a more severe but still similar phenotype to *Pkd1* knockout mice. Of note, we were unable to analyse the mesenteric valves in these *Wnt5a*-null mice due to severe defects in intestinal development at the stages of interest. We observed similar but milder lymphatic defects in $Ryk^{-/-}$ mutants. Both $Wnt5a^{-/-}$ and $Ryk^{-/-}$ mutants had dilated lymphatic vessels,

increased number of cells near the sprout tip and the nuclei were less polarised. However, the *Wnt5a*$^{-/-}$ lymphatic sprouts also had reduced migration distance to midline, which was not observed in *Ryk*$^{-/-}$ mutants (data not shown). It is perhaps not surprising that *Ryk*$^{-/-}$ mutants had milder phenotypes because Ryk is one of many Wnt5a receptors, while Wnt5a is the major ligand of the PCP pathway [41,]reviewed in [42]. In the context of lymphatic valve development, the PCP core components VANGL2 and CELSR1 control valve LEC polarisation and orientation in the mesentery [12]. Coupled with our findings above these similar observations support an important role for the non-canonical WNT/PCP pathway in lymphatic network formation and LEC polarity and a role for *Pkd1* interacting with this pathway.

The question remains, how does PC1 interact with the PCP pathway at a mechanistic level? It seems unlikely that the genetic interaction we report here occurs due to altered Wnt5a expression levels. We saw no change in Wnt5a expression in preliminary transcriptomic analyses (unpublished) and more extensive RNA sequencing analysis of both Pkd1 and Pkd2 knockout mouse kidneys over three different stages of development did not reveal changes in *Wnt5a* transcript levels [43]. PC1 (encoded by *Pkd1*) can directly interact with PCP components at the protein level. PC1 complexes with PAR3 to promote PAR3/aPKC complex formation in mouse embryonic fibroblasts (MEFs) and so it is possible the interaction is also direct in LECs [25]. However, PC1 also complexes with PC2 to form a Ca^{2+} channel and WNT5A can bind and activate the PC1/PC2 complex to induce Ca^{2+} influx [26]. It is currently unclear whether WNT/Ca^{2+} signalling contributes to lymphatic development, although it has been shown that shear stress induces Ca^{2+} pulses in LECs [44,45] and the Ca^{2+} channel ORAI1 is required for trachea and dermal lymphatic development [46]. So it is possible that PC1 may influence Ca2+-dependent WNT signalling, or PCP signalling, or both, to control vessel morphogenesis and the genetic data presented here does not currently distinguish between these possible mechanisms. Of note, canonical WNT signalling is also required for lymphatic development [9]. The deletion of *β-catenin* and the WNT co-receptors *Lrp5* and *Lrp6* from lymphatics leads to lymphatic morphogenesis defects in the dermal vessel network and lymphatic valve formation defects [9,47]. Thus, there appear to be multiple ways in which WNT signalling cascades can influence lymphatic development and the precise role (or roles) of *Pkd1*/PC1 will require further study in the future.

It is likely that both PC1 and PCP components regulate lymphangiogenesis through influencing cell-cell junctions and cytoskeleton. *Pkd1* mutant mice have irregular protrusions of β-catenin and VE-cadherin at the lymphatic cell-cell junctions [27]. *Pkd1* knockdown in human umbilical vascular endothelial cells (HUVECs) also led to disorganised F-ACTIN, β-catenin and VE-CADHERIN [27]. Of note, WNT5A knockdown HUVECs in wound healing assays have disorganised stress fibres that are detached

from adherens junctions, and there were more low-force reticular junctions and less high-force serrated VE-cadherin junctions in these cells [48]. Finally, when human coronary artery endothelial cell (HUAEC) monolayers were treated with WNT5A, the cell-cell junctions were dissociated and β-catenin and VE-CADHERIN were lost, resulting in an acute increase in monolayer permeability [49]. Interestingly, this WNT5A treatment had no effect when *RYK* was also knocked-down [49]. These studies together suggest that both PC1 and PCP components influence endothelial cell-cell junctions and the cytoskeleton, and thus it seems likely that cross-regulation between these proteins could happen at the lymphatic endothelial cell-cell junctions during embryonic development in the contexts described in this study.

Pkd1 is the most commonly mutated gene in autosomal dominant polycystic kidney disease. As such, most emphasis on the role of *Pkd1* in disease has focussed on the kidney. However, this work and our earlier findings suggest that *Pkd1* is a candidate that could influence diseases of the lymphatic vasculature. Of note, in kidney development *Pkd1* also acts by interacting with WNT pathways and the regulation of cell polarity, so there may be common mechanisms at play in both contexts. If PC1 does act via similar mechanisms to FAT4 and DCHS1, given that *Fat4* is mutated in Hennekam syndrome, it will be interesting to explore the interaction between *Fat4* and *Pkd1* and determine if *Pkd1* may modify disease phenotypes in lymphoedema. It will also be interesting to know if *RYK* or *WNT5A* mutations are associated with primary lymphoedema in humans. Overall, this study identified the roles of PC1, WNT5A and RYK in all regulating LEC polarity, and identified additional steps of lymphangiogenesis controlled by *Pkd1* (valve formation in the dermis and mesentery). We found that *Pkd1* and *Wnt5a* genetically interact and suggest that *Pkd1* regulates LEC polarity by influencing the PCP pathway. This work thus provides a deeper understanding of the role of *Pkd1* in lymphatic vascular development and points to potential roles in lymphatic disease.

Experimental Procedures

Animals

Pkd1$^{f/f}$;Cdh5-cre/ERT2 mice were generated by crossing *B6.129S4-Pkd1^{tm2Ggg}/J* (*Pkd1$^{f/f}$*; MGI:97603) mice to *Tg(Cdh5-cre/ERT2)1Rha* (MGI:3848982), and breeding carriers to generate subsequent generations and experimental animals. The breeding strategy for the *Pkd1$^{+/-}$* mouse model used in this study was previously described in [27]. *Wnt5a$^{-/-}$* mice were generated by in-crossing B6;129S7-*Wnt5a^{tm1Amc}/J* (mixed background; MGI:98958). *Pkd1$^{+/-}$* and *Wnt5a$^{+/-}$* were crossed to generate double heterozygous carriers. The carriers were incrossed to produce various genotypes of *Pkd1*;*Wnt5a* double mutants and littermate controls.

Timed pregnancies were set up and adult female mice checked for plugs accordingly. To induce Cre recombination and after pregnancy is confirmed, the female is given a dose of 4-Hydroxytamoxifen (Sigma-Aldrich Cat# H6278) dissolved in 90% sunflower oil/10% Ethanol at a concentration of 10mg/mL, during three consecutive days. Dosing of 40mg per kg of body weight was given by intraperitoneal injection. To excise the floxed alleles in *Pkd1$^{f/f}$;Cdh5-cre/ERT* for the dermal lymphatic model, pregnant females were injected at 9.5dpc, 10.5dpc, and 11.5dpc and, for the mesenteric lymphatic model pregnant females were injected at 15.5dpc, 16.5dpc and 17.5dpc.

Genotyping primer sequences: *Pkd1$^{fl/fl}$*-geno Forward-5'-CCGCCTTGCTCTACTTTCC-3'; *Pkd1$^{fl/fl}$*-geno Reverse-5'-AGGGCTTTTCTTGCTGGTCT-3'; *Cre*-geno Forward-5'-CTGACCGTACACCAAAATTTGCCTG-3'; *Cre*-geno Reverse- 5'-GATAATCGCGAACATCTTCAGGTTC-3'; *Pkd1*-geno Forward-5'-CCTGCCTTGCTCTACTTTCC-3'; *Pkd1*-geno Reverse-5'-TCGTGTTCCCTTACCAACCCTC-3'; *Wnt5a*-geno Forward- 5'-GTTGATTCTGTGTGCCTATTCTGC-3'; *Wnt5a*-geno Reverse1-5'-CCCCGTGGAACTGAGTGTAT-3'; *Wnt5a*-geno Reverse2-5'-TGGA TGTGGAA TGTGTGCGAG-3'. The *Ryk* knock-out mouse breeding and genotyping genotyping was as previously described in [38].

Immunofluorescence staining

Embryos were harvested at 14.5dpc or 16.5dpc and fixed in 4% paraformaldehyde in phosphate buffered saline (PBS) at 4°C overnight and then stored in PBS. Dorsal skins from under ear shell to above hind limb were dissected out from the back of embryos and muscle tissue was removed from the skin as previously described by [31]. The mesenteric membrane was isolated from intestines when harvesting embryos at 18.5dpc. The mesenteric membrane was fixed in 4% paraformaldehyde in PBS at room temperature for 1 hour, and stored in PBS. The skins and mesenteric membranes were

blocked in 10% heat-inactivated horse serum in washing buffer containing 100mM maleic acid, 1% dimethyl sulfoxide and 0.1% Triton-X in PBS for 1 hour at room temperature. After blocking, samples were incubated in blocking buffer with primary antibodies overnight at 4°C. Samples were then washed during the day with washing buffer for 5 hours and then incubated in blocking buffer with secondary antibodies. Samples were washed again with washing buffer throughout the day and mounted with Vectashield Antifade Mounting Medium (Vector Laboratories Cat# H-1000-10) on a clear microscope slide. Various combinations of antibodies were used to achieve co-staining of different proteins. Primary antibodies used were: anti-EMCN (Santa Cruz SC-53941), anti-PROX1 (AngioBio 11-002), anti-NRP2 (R&D System AF567), and anti-GOLPH4 (Abcam ab28049). The following secondary antibodies were used: Donkey anti-Goat IgG (H + L) Cross-Adsorbed, Alexa Fluor 488 (Invitrogen, A11055), Goat anti-Rat IgG (H + L) Cross-Adsorbed, Alexa Fluor 647 (Invi-trogen, A21247), Donkey anti-Rabbit IgG (H + L)Highly Cross-Adsorbed, Alexa Fluor 594 (Invitrogen, A21207), Alexa Fluor 488 Phalloidin (Invitrogen, A12379). Stained skins and mesenteric membranes were mounted on glass slides with gelvatol mounting medium and stored at 4°C until imaging.

Imaging

All mouse embryos were imaged prior to fixation using a Leica M165 FC at 0.73x magnification, illuminated by an external light source. The mounted skins of Figure 1 and 4 were imaged on a Nikon Ti-E Deconvolution Microscope with a 4x Plan Apochromat N.A. 0.2 objective to generate skin scan images for quantifications of lymphatic network formation. The mounted skins and mesenteries of Figure 1 and 4 were imaged on a Zeiss LSM 710 Meta Confocal Scanner with 40x Oil Plan Apochromat N.A. 1.3 and 63x Oil Plan Apochromat N.A. 1.4 objectives to generate vessel images for quantifications all cellular level. The mounted skin of Figure 3 and 4 were imaged with a Zeiss LSM 510 or Zeiss LSM 710 Meta Confocal Scanner with 40x Oil Plan Apochromat N.A. 1.3 and 63x Oil Plan Apochromat N.A. 1.4 objectives.

Quantification and image analysis

All images were analysed with Fiji [50]. We quantified all branch points and loops of the subcutaneous lymphatic network within 2000µm from the midline in 13.5dpc and 14.5dpc embryos. We randomly selected 5 lymphatic sprouts from each side of the dermal lymphatics, and quantified the ellipticity of 10 nuclei in 14.5dpc embryos in **Figure 1, 2 and 4**. We quantified the number of branch points and lymphatic valves of the subcutaneous lymphatic network within 2000µm from the midline in 16.5dpc embryos for **Figure 1**. We quantified the orientation and nuclei ellipticity (nuclei length-to-width ratio) for the lymphatic valve nuclei that showed upregulated PROX1 (1.5 times of mean fluorescent

intensity) for **Figure 1**. We analysed 5 valves on the primary spokes of mesenteries from each embryo at 18.5dpf that were stained for F-Actin using Phalloidin, lymphatics using PROX1 and veins using EMCN. Since lymphatic valve cells have an upregulation of PROX1 [51], all Prox1 upregulated valve nuclei (1.5 times of mean fluorescent intensity) from each valve were quantified for nuclei ellipticity in **Figure 1**. The intensity of F-Actin and PROX1 staining in **Figure 1** was measured from the centre Z-section of each Z-stack through each valve based on the location of the nucleus. The ratio of valve to lymphatic vessel mean F-actin staining intensity was calculated. We selected 5 vessels from each side of the skin for the quantification of genetic interaction at a cellular level in **Figure 2-4**. We used NRP2 expression as a mask to remove non-endothelial Golph4 staining, and measured the angle between the Golgi body, the nuclei and the tip of lymphatic sprout in **Figure 2**. We measured the width of the selected vessels at 10, 25, 50, 75, 100µm from the tip of lymphatic sprouts, and the average width of the 5 measurements was considered as the width of the vessel. The number of LECs in the vessel tip were counted on 5 lymphatic sprouts on each side of the dermal lymphatics in **Figure 4**. All quantifications were done genotype blinded.

Statistical analysis

We performed all statistical tests and generated all dot plots using GraphPad Prism 7 except for the rose diagram generated using PAST [52]. Specific tests used in each experiment are indicated in the figure legend.

Acknowledgements

This work was supported by National Health and Medical Research Council of Australia (NHMRC) grants 1079158 and 1146352. BMH was supported by a fellowship (1155221) from the NHMRC. SAS. was supported by an NHMRC Program Grant (1053535), an NHMRC Senior Research Fellowship (1154746) and an NHMRC Investigator Grant (1176732) and by funds from the Operational Infrastructure Support Program provided by the Victorian Government,

We thank Dr. Kelly Betterman for their help with mesenteric lymphatic staining protocols. All images were acquired at the Australian Cancer Research Foundation's Dynamic Imaging Facility at the Institute for Molecular Biosciences.

Competing interests

No competing interests declared.

Funding

NHMRC grants 1079158, 1146352, 1053535. NHMRC fellowships 1155221, 1154746, 1176732.

Data availability

No publicly available dataset used.

References

1. Koltowska K, Betterman KL, Harvey NL, Hogan BM. Getting out and about: the emergence and morphogenesis of the vertebrate lymphatic vasculature. *Development*. 2013;140(9):1857-1870. https://doi.org10.1242/dev.089565.
2. Francois M, Caprini A, Hosking B, et al. Sox18 induces development of the lymphatic vasculature in mice.(LETTERS)(Report). *Nature*. 2008;456(7222):643. https://doi.org10.1038/nature07391.
3. Oliver G, Srinivasan RS. Endothelial cell plasticity: how to become and remain a lymphatic endothelial cell. *Development*. Feb 2010;137(3):363-72. https://doi.org10.1242/dev.035360.
4. Wigle JT, Oliver G. Prox1 function is required for the development of the murine lymphatic system. *Cell*. Sep 17 1999;98(6):769-78.
5. Hägerling R, Pollmann C, Andreas M, et al. A novel multistep mechanism for initial lymphangiogenesis in mouse embryos based on ultramicroscopy. *EMBO journal: European Molecular Biology Organization*. 2013;(5):629-644.
6. Yang Y, Garcia-Verdugo JM, Soriano-Navarro M, et al. Lymphatic endothelial progenitors bud from the cardinal vein and intersomitic vessels in mammalian embryos. *Blood*. Sep 13 2012;120(11):2340-8. https://doi.org10.1182/blood-2012-05-428607.
7. Karkkainen M, Haiko P, Sainio K, et al. Vascular endothelial growth factor C is required for sprouting of the first lymphatic vessels from embryonic veins. *Nature Immunology*. 2004;5(1):74-80. https://doi.org10.1038/ni1013.
8. Buttler K, Becker J, Pukrop T, Wilting J. Maldevelopment of dermal lymphatics in Wnt5a-knockout-mice. *Developmental Biology*. 2013;381(2):365-376. https://doi.org10.1016/j.ydbio.2013.06.028.
9. Cha B, Geng X, Mahamud MR, et al. Complementary Wnt Sources Regulate Lymphatic Vascular Development via PROX1-Dependent Wnt/β-Catenin Signaling. *Cell Rep*. 2018;25(3):571-584.e5. https://doi.org10.1016/j.celrep.2018.09.049.
10. Lutze G, Haarmann A, Demanou Toukam JA, Buttler K, Wilting J, Becker J. Non-canonical WNT-signaling controls differentiation of lymphatics and extension lymphangiogenesis via RAC and JNK signaling. *Scientific reports*. 2019;9(1):4739-4739. https://doi.org10.1038/s41598-019-41299-7.
11. Cha B, Geng X, Mahamud MR, et al. Mechanotransduction activates canonical Wnt/β-catenin signaling to promote lymphatic vascular patterning and the development of lymphatic and lymphovenous valves. *Genes Dev*. 2016;30(12):1454-1469. https://doi.org10.1101/gad.282400.116.
12. Tatin F, Taddei A, Weston A, et al. Planar Cell Polarity Protein Celsr1 Regulates Endothelial Adherens Junctions and Directed Cell Rearrangements during Valve Morphogenesis. *Developmental Cell*. 2013;26(1):31-44. https://doi.org10.1016/j.devcel.2013.05.015.
13. Keeble TR, Halford MM, Seaman C, et al. The Wnt receptor Ryk is required for Wnt5a-mediated axon guidance on the contralateral side of the corpus callosum. *The Journal of neuroscience : the official journal of the Society for Neuroscience*. 2006;26(21):5840-5848. https://doi.org10.1523/JNEUROSCI.1175-06.2006.
14. Lu W, Yamamoto V, Ortega B, Baltimore D. Mammalian Ryk Is a Wnt Coreceptor Required for Stimulation of Neurite Outgrowth. *Cell*. 2004;119(1):97-108. https://doi.org10.1016/j.cell.2004.09.019.
15. Roy JP, Halford MM, Stacker SA. The biochemistry, signalling and disease relevance of RYK and other WNT-binding receptor tyrosine kinases. *Growth factors (Chur, Switzerland)*. 2018;36(1-2):15-40. https://doi.org10.1080/08977194.2018.1472089.

16. Butler MT, Wallingford JB. Planar cell polarity in development and disease. *Nat Rev Mol Cell Biol*. 2017;18(6):375-388. https://doi.org10.1038/nrm.2017.11.
17. Cadigan KM, Waterman ML. TCF/LEFs and Wnt Signaling in the Nucleus. *Cold Spring Harb Perspect Biol*. 2012;4(11):a007906-a007906. https://doi.org10.1101/cshperspect.a007906.
18. Peters DJM, Sandkuijl LA. Genetic Heterogeneity of Polycystic Kidney Disease in Europe. *Contributions to Nephrology*. 1992:128-139. https://doi.org10.1159/000421651.
19. Hughes J, Ward CJ, Peral B, et al. The polycystic kidney disease 1 (PKD1) gene encodes a novel protein with multiple cell recognition domains. *Nat Genet*. 1995;10(2):151-160. https://doi.org10.1038/ng0695-151.
20. Nims N, Vassmer D, Maser RL. Transmembrane Domain Analysis of Polycystin-1, the Product of the Polycystic Kidney Disease-1 (PKD1) Gene: Evidence for 11 Membrane-Spanning Domains. *Biochemistry*. 2003;42(44):13035-13048. https://doi.org10.1021/bi035074c.
21. Nauli SM, Alenghat FJ, Luo Y, et al. Polycystins 1 and 2 mediate mechanosensation in the primary cilium of kidney cells. *Nat Genet*. 2003;33(2):129-137. https://doi.org10.1038/ng1076.
22. Yoder BK, Hou X, Guay-Woodford LM. The Polycystic Kidney Disease Proteins, Polycystin-1, Polycystin-2, Polaris, and Cystin, Are Co-Localized in Renal Cilia. *J Am Soc Nephrol*. 2002;13(10):2508-2516. https://doi.org10.1097/01.asn.0000029587.47950.25.
23. Hanaoka K, Qian F, Boletta A, et al. Co-assembly of polycystin-1 and -2 produces unique cation-permeable currents. *Nature*. 2000;408(6815):990-994. https://doi.org10.1038/35050128.
24. Vassilev PM, Guo L, Chen X-Z, et al. Polycystin-2 Is a Novel Cation Channel Implicated in Defective Intracellular Ca2+ Homeostasis in Polycystic Kidney Disease. *Biochemical and biophysical research communications*. 2001;282(1):341-350. https://doi.org10.1006/bbrc.2001.4554.
25. Castelli M, Boca M, Chiaravalli M, et al. Polycystin-1 binds Par3/aPKC and controls convergent extension during renal tubular morphogenesis. *Nature Communications*. 2013;4(1):2658. https://doi.org10.1038/ncomms3658.
26. Kim S, Nie H, Nesin V, et al. The polycystin complex mediates Wnt/Ca2+ signalling. *Nature Cell Biology*. 2016;18(7):752-764. https://doi.org10.1038/ncb3363.
27. Coxam B, Sabine A, Bower Neil i, et al. Pkd1 Regulates Lymphatic Vascular Morphogenesis during Development. *Cell Reports*. 2014;7(3):623-633. https://doi.org10.1016/j.celrep.2014.03.063.
28. Outeda P, Huso David L, Fisher Steven A, et al. Polycystin Signaling Is Required for Directed Endothelial Cell Migration and Lymphatic Development. *Cell Rep*. 2014;7(3):634-644. https://doi.org10.1016/j.celrep.2014.03.064.
29. Alva JA, Zovein AC, Monvoisin A, et al. VE-Cadherin-Cre-recombinase transgenic mouse: A tool for lineage analysis and gene deletion in endothelial cells. *Developmental Dynamics*. 2006;235(3):759-767. https://doi.org10.1002/dvdy.20643.
30. Sörensen I, Adams RH, Gossler A. DLL1-mediated Notch activation regulates endothelial identity in mouse fetal arteries. *Blood*. 2009;113(22):5680-5688. https://doi.org10.1182/blood-2008-08-174508.
31. James JM, Nalbandian A, Mukouyama Y-s. TGFβ signaling is required for sprouting lymphangiogenesis during lymphatic network development in the skin. *Development*. 2013;140(18):3903-3914. https://doi.org10.1242/dev.095026.
32. Sabine A, Davis MJ, Bovay E, Petrova TV. Characterization of Mouse Mesenteric Lymphatic Valve Structure and Function. *Lymphangiogenesis*. 2018;1846:97-129. https://doi.org10.1007/978-1-4939-8712-2_7.
33. Kume T. Lymphatic vessel development: fluid flow and valve-forming cells. *J Clin Invest*. 2015;125(8):2924-2926. https://doi.org10.1172/JCI83189.

34. Betterman KL, Sutton DL, Secker GA, et al. Atypical cadherin FAT4 orchestrates lymphatic endothelial cell polarity in response to flow. *The Journal of clinical investigation*. 2020;130(6):3315-3328. https://doi.org10.1172/JCI99027.
35. Norden PR, Sabine A, Wang Y, et al. Shear stimulation of FOXC1 and FOXC2 differentially regulates cytoskeletal activity during lymphatic valve maturation. *Elife*. 2020;9. https://doi.org10.7554/eLife.53814.
36. Andre P, Wang Q, Wang N, et al. The Wnt Coreceptor Ryk Regulates Wnt/Planar Cell Polarity by Modulating the Degradation of the Core Planar Cell Polarity Component Vangl2. *J Biol Chem*. 2012;287(53):44518-44525. https://doi.org10.1074/jbc.M112.414441.
37. Macheda ML, Sun WW, Kugathasan K, et al. The Wnt Receptor Ryk Plays a Role in Mammalian Planar Cell Polarity Signaling. *J Biol Chem*. 2012;287(35):29312-29323. https://doi.org10.1074/jbc.m112.362681.
38. Halford MM, Armes J, Buchert M, et al. Ryk-deficient mice exhibit craniofacial defects associated with perturbed Eph receptor crosstalk. *Nat Genet*. 2000;25(4):414-418. https://doi.org10.1038/78099.
39. Alders M, Al-Gazali L, Cordeiro I, et al. Hennekam syndrome can be caused by FAT4 mutations and be allelic to Van Maldergem syndrome. *Hum Genet*. 2014;133(9):1161-1167. https://doi.org10.1007/s00439-014-1456-y.
40. Pujol F, Hodgson T, Martinez-Corral I, et al. Dachsous1–Fat4 Signaling Controls Endothelial Cell Polarization During Lymphatic Valve Morphogenesis—Brief Report. *Arterioscler Thromb Vasc Biol*. 2017;37(9):1732-1735. https://doi.org10.1161/ATVBAHA.117.309818.
41. Hsieh JC, Kodjabachian L, Rebbert ML, et al. A new secreted protein that binds to Wnt proteins and inhibits their activities. *Nature*. 1999;398(6726):431-436.
42. Niehrs C. The complex world of WNT receptor signalling. *Nat Rev Mol Cell Biol*. 2012;13(12):767-779. https://doi.org10.1038/nrm3470.
43. Woo YM, Kim DY, Koo NJ, et al. Profiling of miRNAs and target genes related to cystogenesis in ADPKD mouse models. *Sci Rep*. Oct 26 2017;7(1):14151. https://doi.org10.1038/s41598-017-14083-8.
44. Surya VN, Michalaki E, Fuller GG, Dunn AR. Lymphatic endothelial cell calcium pulses are sensitive to spatial gradients in wall shear stress. *Mol Biol Cell*. 2019;30(7):923-931. https://doi.org10.1091/mbc.E18-10-0618.
45. Choi D, Park E, Jung E, et al. Laminar flow downregulates Notch activity to promote lymphatic sprouting. *J Clin Invest*. 2017;127(4):1225-1240. https://doi.org10.1172/jci87442.
46. Choi D, Park E, Jung E, et al. ORAI1 Activates Proliferation of Lymphatic Endothelial Cells in Response to Laminar Flow Through Krüppel-Like Factors 2 and 4. *Circ Res*. 2017;120(9):1426-1439. https://doi.org10.1161/CIRCRESAHA.116.309548.
47. Cha B, Geng X, Mahamud MR, et al. Mechanotransduction activates canonical Wnt/beta-catenin signaling to promote lymphatic vascular patterning and the development of lymphatic and lymphovenous valves. *Genes Dev*. Jun 15 2016;30(12):1454-69. https://doi.org10.1101/gad.282400.116.
48. Carvalho JR, Fortunato IC, Fonseca CG, et al. Non-canonical Wnt signaling regulates junctional mechanocoupling during angiogenic collective cell migration. *Elife*. 2019;8. https://doi.org10.7554/eLife.45853.
49. Skaria T, Bachli E, Schoedon G. Wnt5A/Ryk signaling critically affects barrier function in human vascular endothelial cells. *Cell Adh Migr*. 2017;11(1):24-38. https://doi.org10.1080/19336918.2016.1178449.
50. Schindelin J, Arganda-Carreras I, Frise E, et al. Fiji: an open-source platform for biological-image analysis. *Nature Methods*. 2012;9(7):676. https://doi.org10.1038/nmeth.2019.
51. Srinivasan RS, Oliver G. Prox1 dosage controls the number of lymphatic endothelial cell progenitors and the formation of the lymphovenous valves. *Genes & development*. 2011;25(20):2187-2197. https://doi.org10.1101/gad.16974811.

52. Hammer Ø, Harper DAT, Ryan PD. Past: Paleontological statistics software package for education and data analysis. *Palaeontologia Electronica*. 2001;4(1):XIX-XX.

FIGURE LEGENDS

Figure 1. *Pkd1* endothelial cell-autonomously regulates subcutaneous lymphatic network and lymphatic valve formation in mice.

(A-B) The overall morphology of *Wt* and *Pkd1*^{iECKO} mouse embryos at 14.5dpc. Scale bar represents 2mm.
(C and D) Subcutaneous lymphatic networks in *Wt* and *Pkd1*^{iECKO} embryos at 14.5dpc stained with NRP2 (grey) and EMCN (magenta). Scale bar represents 1000µm.
(C' and D') Subcutaneous blood vessels in *Wt* and *Pkd1*^{iECKO} embryos at 14.5dpc stained with EMCN. Scale bar represents 1000µm.
(E-F) Subcutaneous lymphatic sprouts in *Wt* and *Pkd1*^{iECKO} embryos at 14.5dpc stained with NRP2 (grey) and PROX1 (green). Scale bar represents 50µm.
(G-I) Quantification of (G) the number of branch points and (H) loops per mm^2, (I) distance of lymphatic sprouts from the midline (µm) in *Wt* (n=6) and *Pkd1*^{iECKO} (n=8) embryos at 14.5dpc.
(J-K) Quantification of (J) the number of branch points and (K) loops per mm^2 of the subcutaneous blood vessels in *Wt* (n=6) and *Pkd1*^{iECKO} (n=8) embryos at 14.5dpc.
(L-M) Subcutaneous lymphatic networks in *Wt* and *Pkd1*^{iECKO} embryos at 16.5dpc stained with NRP2 (grey) and PROX1 (green). Scale bar represents 1000µm. Arrows indicate developing lymphatic valve territories.
(L'-M') Magnification of the dermal lymphatic valves in *Wt* and *Pkd1*^{iECKO} embryos at 16.5dpc with PROX1 staining. Scale bars represent 50µm.
(N-O) Quantification of (N) the number of valves per branch point, and (O) the ratio of polarised valves to unpolarised valves in *Wt* (n=3) and *Pkd1*^{iECKO} (n=3) embryos subcutaneous lymphatics at 16.5dpc.
(P-Q'') Mesenteric lymphatic valves in *Wt* and *Pkd1*^{iECKO} embryos at 18.5dpc stained with Phalloidin (grey) and PROX1 (green). Scale bars represent 50µm. (P' and Q') *Wt* and *Pkd1*^{iECKO} valves stained with PROX1 and (P"-Q") stained with Phalloidin. Scale bars represent 5µm.
(R-S) Quantification for (R) nuclei ellipticity and (S) valve to vessel actin fluorescent intensity ratio in *Wt* (n=5) and *Pkd1*^{iECKO} (n=6) embryos at 18.5dpc.
Mean±s.e.m. are shown. Student's *t*-test. ****: p-value<0.0001, ***: p-value<0.001, **: p-value<0.01, *: p-value<0.05

Figure 2. Wnt5a mutant mice display dermal lymphatic network polarity defects

(A-B) Subcutaneous lymphatic networks in *Wnt5a*$^{+/+}$ and *Wnt5a*$^{-/-}$ mouse embryos at 13.5dpc stained with NRP2 (grey) and EMCN (magenta). Scale bar represents 1000µm.
(A'-B') Subcutaneous blood vessel networks in *Wnt5a*$^{+/+}$ and *Wnt5a*$^{-/-}$ mouse embryos at 13.5dpc stained with EMCN. Scale bar represents 1000µm.
(C-F) Quantification of (C) vessel width, (D) distance from midline, (E) the number of nuclei/150µm vessel, and (F) nuclei ellipticity of subcutaneous lymphatic vessel networks in *Wnt5a*$^{+/+}$ (n=5) and *Wnt5a*$^{-/-}$ (n=5) embryos at 13.5dpc.
(G and H) Subcutaneous lymphatic sprouts in *Wnt5a*$^{+/+}$ and *Wnt5a*$^{-/-}$ mouse embryos at 13.5dpc stained with PROX1 and GOLPH4. Scale bar represents 50µm.
(G'and H') Magnification of a nucleus and its Golgi body in the stained subcutaneous lymphatic sprouts. Scale bar represents 5µm.
(I-K) Quantification of Golgi body position relative to the migration direction of lymphatic sprouts to determine cell polarity in *Wnt5a*$^{+/+}$ (n=5) and *Wnt5a*$^{-/-}$ (n=5) mouse embryos at 13.5 dpc.
(L-M) Quantification of (L) the number of branch points and (M) the number of loops of subcutaneous blood vessel networks in *Wnt5a*$^{+/+}$ (n=5) and *Wnt5a*$^{-/-}$ (n=5) embryos at 13.5dpc.
Mean±s.e.m. are shown. Student's *t*-test. ****: p-value<0.0001, ***: p-value<0.001, **: p-value<0.01, *: p-value<0.05

Figure 3. Ryk is required for subcutaneous lymphatic vascular morphogenesis

(A-B) Subcutaneous lymphatic networks in *Ryk*$^{+/+}$ and *Ryk*$^{-/-}$ mouse embryos at 14.5dpc stained with NRP2 (grey), PROX1 (green) and EMCN (magenta). Scale bar represents 1000µm.
(A'-B') Subcutaneous blood vessel networks in *Ryk*$^{+/+}$ and *Ryk*$^{-/-}$ mouse embryos at 14.5dpc stained with EMCN. Scale bar represents 1000µm.
(C-D) Subcutaneous lymphatic sprouts in *Ryk*$^{+/+}$ and *Ryk*$^{-/-}$ mouse embryos at 14.5dpc stained with NRP2 (grey) and PROX1 (green). Scale bar represents 50µm.
(E-G) Quantification of (E) nuclei ellipticity, (F)vessel width and (G) the number of nuclei/100µm vessel of subcutaneous lymphatic vessel networks in *Ryk*$^{+/+}$ (n=5) and *Ryk*$^{-/-}$ (n=5) mouse embryos at 14.5dpc.
(H-I) Quantification of (H) the number of branch points and (I) loops of subcutaneous blood vessel networks in *Ryk*$^{+/+}$ (n=5) and *Ryk*$^{-/-}$ (n=5) mouse embryos at 14.5dpc.
Mean±s.e.m. are shown. Student's *t*-test. ****: p-value<0.0001, ***: p-value<0.001, **: p-value<0.01, *: p-value<0.05

Figure 4. Pkd1 and Wnt5a double mutants show less severe lymphatic defects than single mutants

(A-F) Subcutaneous lymphatic networks in (A) *Wt* , (B) *Pkd1*$^{-/-}$, (C) *Wnt5a*$^{-/-}$, (D) *Pkd1*$^{-/-}$;*Wnt5a*$^{-/-}$, (E) *Pkd1*$^{-/-}$;*Wnt5a*$^{+/-}$, and (F) *Pkd1*$^{+/-}$;*Wnt5a*$^{-/-}$, mouse embryos at 14.5dpc stained with NRP2 (grey) and EMCN (magenta). Scale bar represents 1000µm.

(A'-F') Subcutaneous blood vessel networks in *Wt*, *Pkd1*$^{-/-}$, *Wnt5a*$^{-/-}$, *Pkd1*$^{-/-}$;*Wnt5a*$^{+/-}$, *Pkd1*$^{-/-}$;*Wnt5a*$^{-/-}$, *Pkd1*$^{+/-}$;*Wnt5a*$^{-/-}$, *Pkd1*$^{-/-}$;*Wnt5a*$^{-/-}$ mouse embryos at 14.5dpc stained with EMCN. Scale bar represents 1000µm.

(G-L) Subcutaneous lymphatic sprouts in (G) *Wt*, (H) *Pkd1*$^{-/-}$, (I) *Wnt5a*$^{-/-}$, (J) *Pkd1*$^{-/-}$;*Wnt5a*$^{-/-}$, (K) *Pkd1*$^{-/-}$;*Wnt5a*$^{+/-}$ and (L) *Pkd1*$^{+/-}$;*Wnt5a*$^{-/-}$, mouse embryos at 14.5dpc stained with NRP2 (grey) and PROX1 (green). Scale bar represents 50µm.

(G'-L') Subcutaneous lymphatic sprouts in *Wt*, *Pkd1*$^{-/-}$, *Wnt5a*$^{-/-}$, *Pkd1*$^{-/-}$;*Wnt5a*$^{-/-}$, *Pkd1*$^{-/-}$;*Wnt5a*$^{+/-}$, *Pkd1*$^{+/-}$;*Wnt5a*$^{-/-}$, mouse embryos at 14.5dpc stained with PROX1.

Figure 5. Quantification of Pkd1 and Wnt5a single and double mutant phenotypes

(A-D) Quantification of number of (A) vessel width, (B) the number of nuclei/100μm vessel, (C) nuclei ellipticity, and (P) number of LECs at the sprout tips of subcutaneous lymphatic vessels.
(E-F) Quantification of (E) the number of branch points and (F) loops per mm^2 of subcutaneous blood vessel networks.
(n*Wt*=6, n*Pkd1*$^{+/-}$=8, n*Wnt5a*$^{+/-}$=5, n*Pkd1*$^{-/-}$=5, n*Wnt5a*$^{-/-}$=6, n*Pkd1*$^{-/-}$;*Wnt5a*$^{+/-}$=8, n*Pkd1*$^{+/-}$;*Wnt5a*$^{-/-}$=4, n*Pkd1*$^{-/-}$;*Wnt5a*$^{-/-}$=4)
Mean±s.e.m. are shown. One-way ANOVA, Tukey's multiple comparisons test. ****: p-value<0.0001, ***: p-value<0.001, **: p-value<0.01, *: p-value<0.05

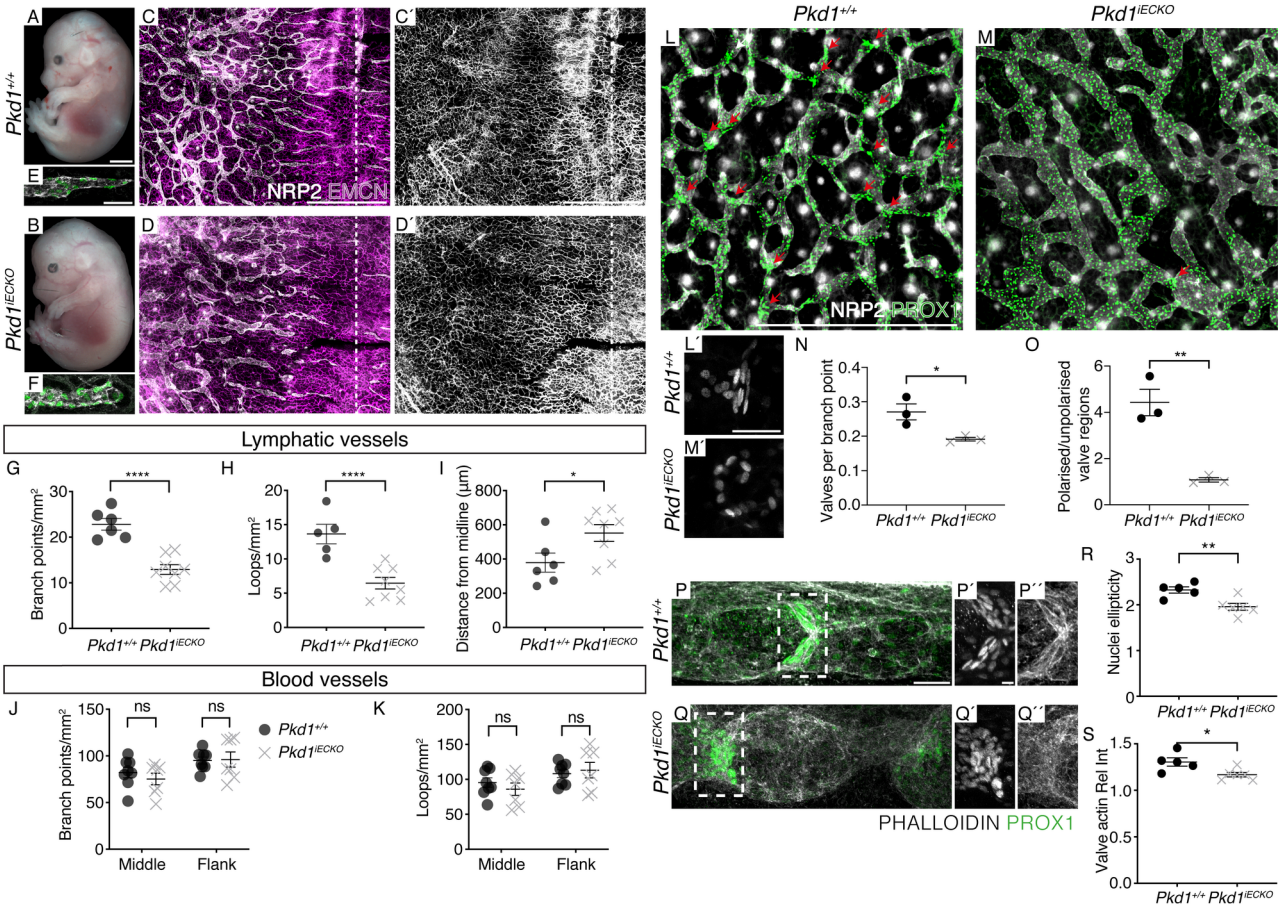

DVDY_390_DVDY_390_Figure1 copy.tif

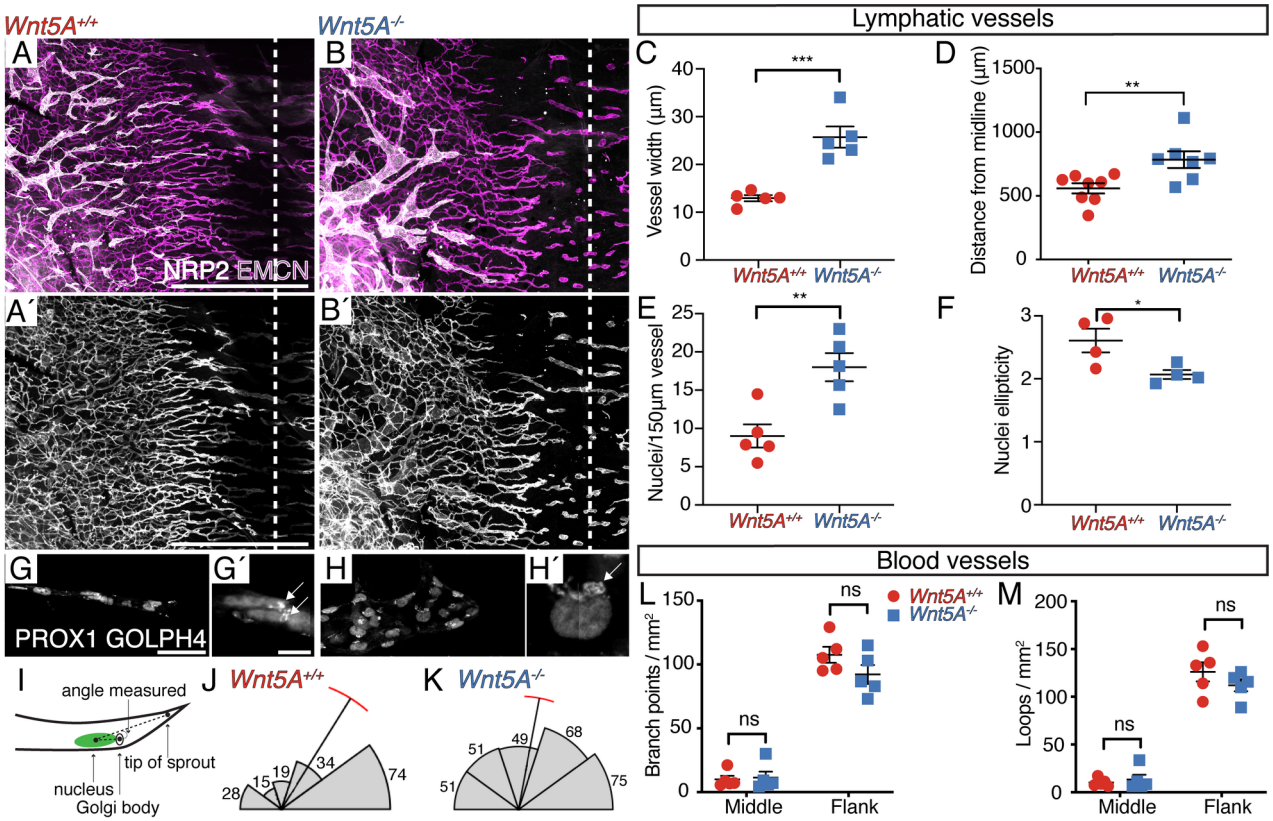

DVDY_390_DVDY_390_Figure2 copy.tif

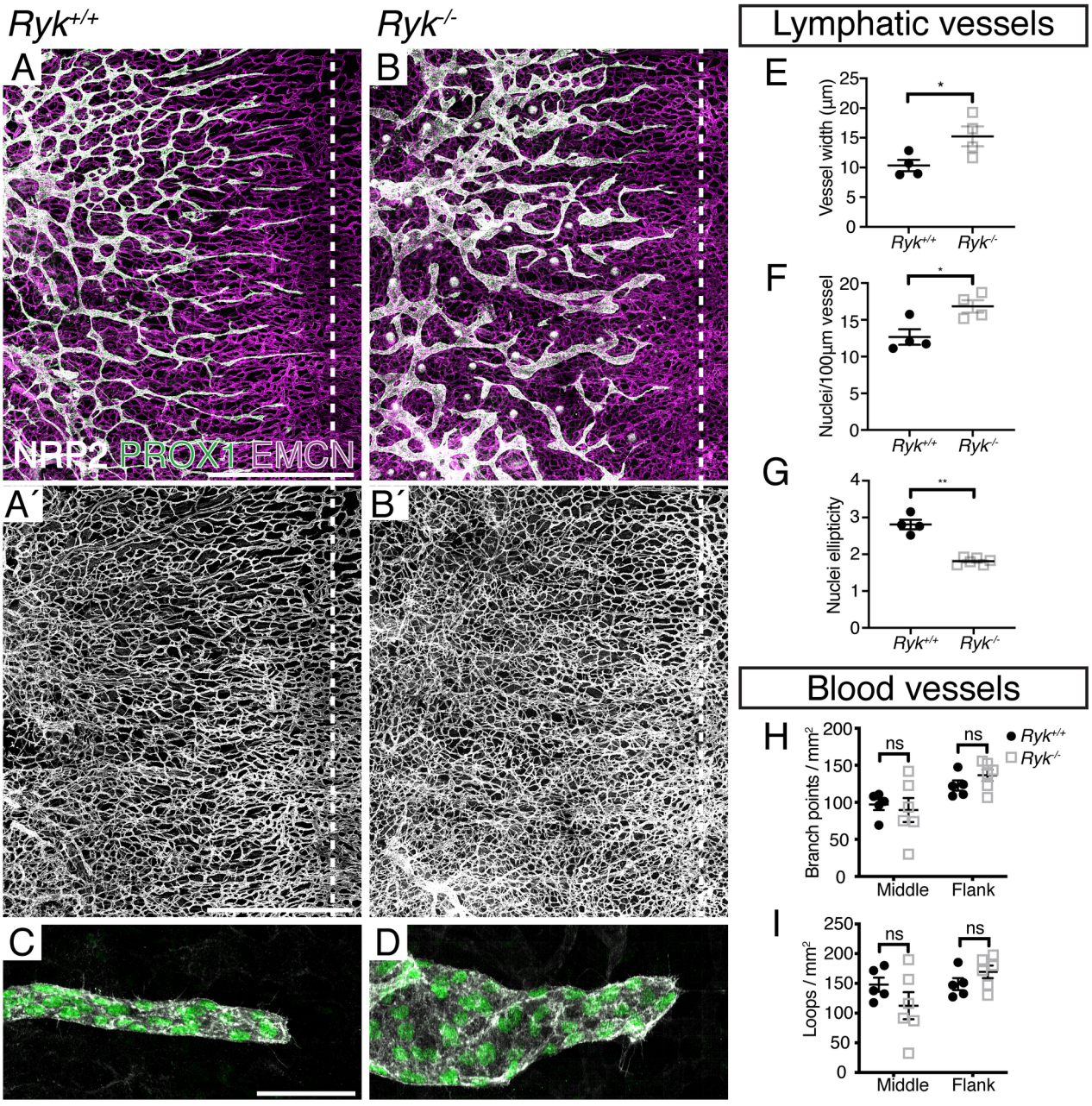

DVDY_390_DVDY_390_Figure 3 copy.tif

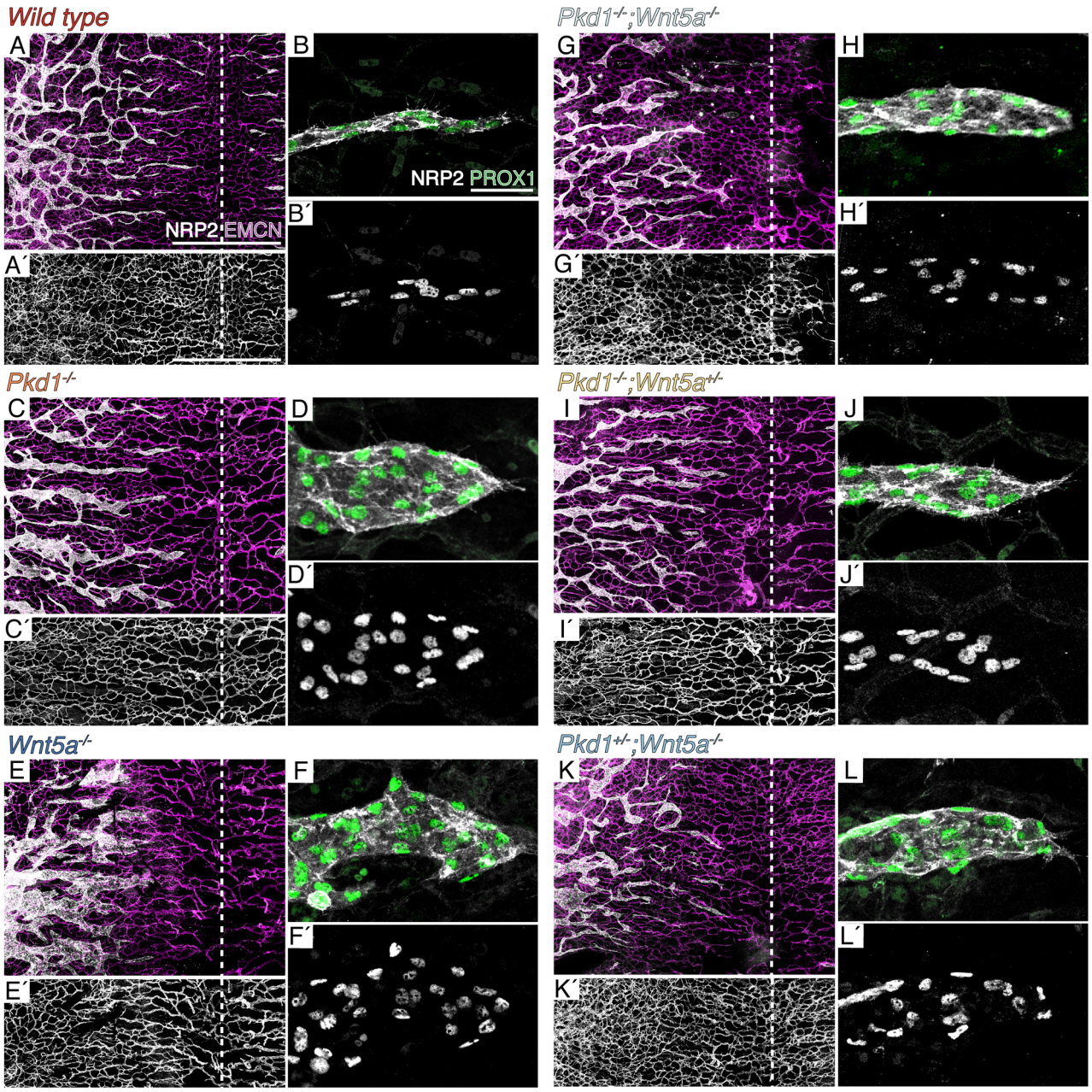

DVDY_390_DVDY_390_Figure 4 copy.tif

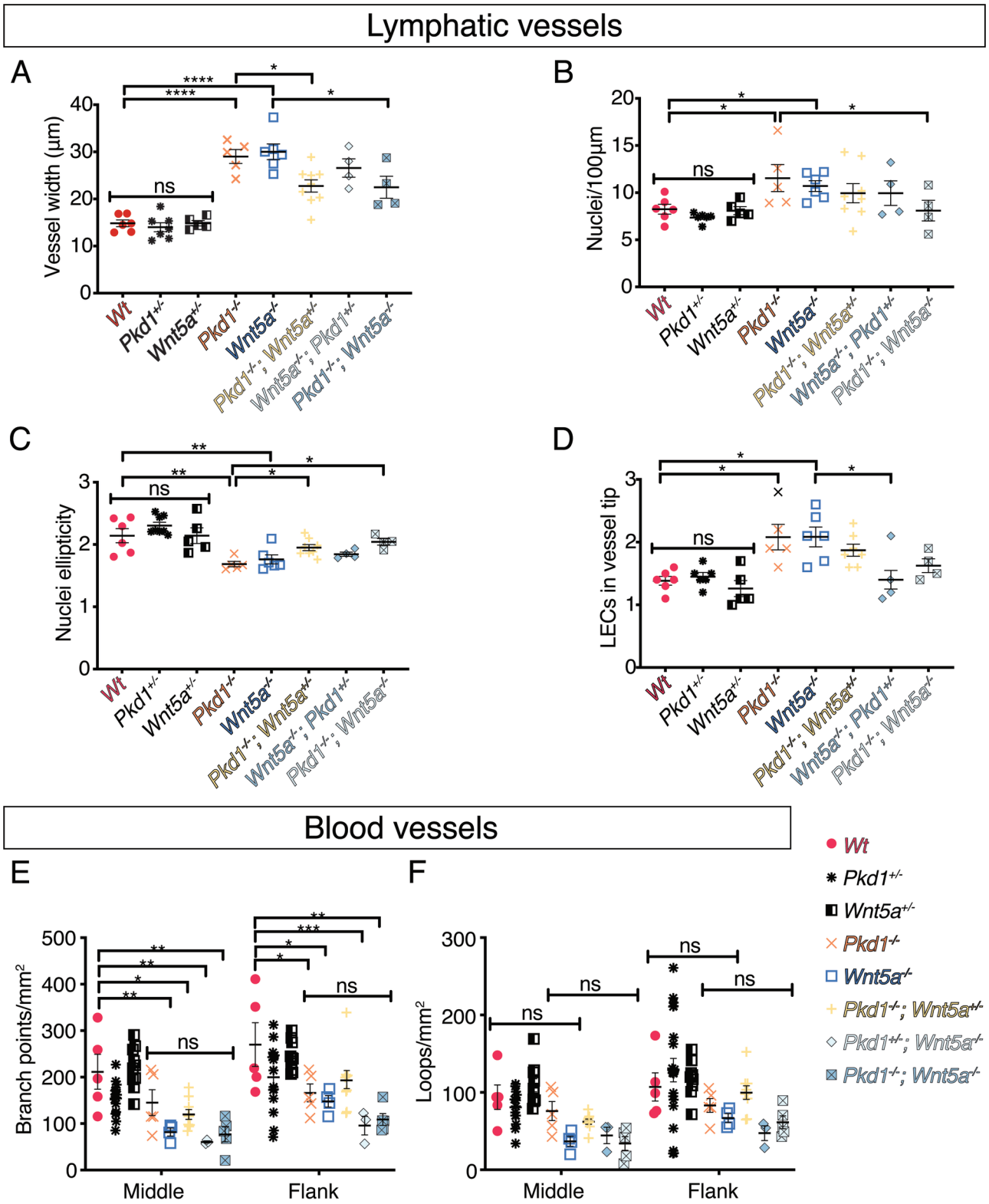

DVDY_390_DVDY_390_Figure 5 copy.tif